Tunneling Behaviors of Photogenerated Electrons in $In_{0.15}Ga_{0.85}As/GaAs$ Quantum Well Photoelectrodes

Yao Liu and Xu-Rui Xiao*

Laboratory of Photochemistry, Center for Molecular Sciences, Institute of Chemistry, Chinese Academy of Sciences, Beijing 100083, China

Yi-Ping Zeng and Dong Pan

Institute of Semiconductors, Chinese Academy of Sciences, Beijing 100083, China

Received: March 26, 1999; In Final Form: September 15, 1999

The photovoltaic spectral features and the behaviors of photocurrent versus the electrode potential for near surface $In_{0.15}Ga_{0.85}As/GaAs$ quantum well electrodes have been investigated in nonaqueous solutions of ferrocene and acetylferrocene. The photovoltaic spectrum shows a sharp structure that reflects confined state-to-state exciton transition in the quantum well. Deep dips are observed in the photocurrent versus the electrode potential curves in both electrolytes at the different electrode potentials under the illumination of exciton resonance wavelength. These dips are qualitatively explained by considering the interfacial tunneling transfer of photogenerated electron within the quantum well.

Introduction

Quantum wells (QWs) and superlattices (SLs) have drawn much attention in semiconductor physics research and semiconductor-based device development due to their unusual physical properties arising from the energy quantizations and engineered electronic structures.[1,2] A multiple quantum well (MQW) semiconductor used in a solar cell has proved to be in possession of higher conversion efficiency than a bulk semiconductor in the lattice-matched GaAs/(AlGa)As system.[3−6] Nozik et al. first introduced the superlattice and quantum well electrodes as new kinds of semiconductor photoelectrodes into photoelectrochemical studies.[7−13] They studied the quantum confined effect of photoelectrodes and hot electron transfer at a p-doped strained layer or lattice-matched SLs/electrolyte interface, which can dramatically improve the conversion efficiency of the semiconductor photovoltaic cell.[14] Recently, using the tailored band structure of QW, the thermodynamic and dynamic characteristics at the surface of QW electrodes were extensively investigated. Diol et al. pointed out that the electron transfer at the semiconductor/outer-sphere acceptor interface is in the adiabatic coupling regime through a study of a GaAs surface quantum well.[15] Liu et al. used a near surface $Al_xGa_{1-x}As/GaAs$ quantum well as a probe to study the interfacial electric field distribution, the interaction between the surface states and adsorbates, and the quantum-confined Stark effects induced by surface interaction.[16−20] In this work, we have studied the photocurrent characteristics of strained $In_xGa_{1-x}As/GaAs$ QW electrodes in contact with nonaqueous electrolytes in order to understand the interfacial behavior of the photogenerated carriers confined in quantum well. Deep dips in the photocurrent vs potential curves were found in our experiments, indicating the existence of tunneling interfacial transfer of photogenerated electrons.

Experimental Section

The near surface $In_{0.15}Ga_{0.85}As/GaAs$ QW was grown on n^+-GaAs(100) substrate coated with a 0.2 μm n-GaAs buffer epilayer (Si doped, 5×10^{16} cm^{-3}) by molecular beam epitaxy (MBE). The detailed layer structure of a double single-quantum-well (DSQW) electrode, from the GaAs epilayer up, is a 7.6 nm undoped $In_{0.15}Ga_{0.85}As$ narrow quantum well layer, a 0.4 μm undoped GaAs barrier layer, and a 9.8 nm undoped $In_{0.15}Ga_{0.85}As$ wide quantum well layer. The outermost layer is a 10 nm GaAs capped layer. The unintentionally doped concentration of undoped epilayer was ca. 1×10^{15} cm^{-3} (n-type). The crystal quality of samples was checked by double crystal X-ray diffraction. The fine satellite structures of diffraction were obtained, indicating a perfect crystal quality.

The QW photoelectrodes prepared by the conventional method with the surface area of 5−7 mm^2 were studied without surface pretreatment. The electrolytes were acetonitrile solution containing 0.1 M tetrabutylammonium tetrafluoroborate and 1×10^{-2} M ferrocene (Fc) or acetylferrocene (AcFc). The concentration of oxidized species in both electrolytes was 1×10^{-3} M, as obtained by electrolysis of Fc and AcFc. Acetonitrile (initial water content <50 ppm, supplied by Aldrich) was dehydrated with an activated 3 Å molecular sieve. The electrolytes were deaerated with pure nitrogen and intensely stirred during the measurements. The photoelectrochemical cell was a three-electrode system with a Ag/AgCl electrode as a reference electrode and 4 cm^2 Pt foil as a counter electrode. The $I-V$ curves were performed using a multichannel ECO Chemie Autolab/GPES electrochemical interface. Photocurrent responses were measured under monochromatic light produced by a xenon lamp through a Schoeffel GM 252 monochromator. The incident photon flux was measured using a UDT Instrument model 360 optometer and a UDT Instrument model 221 calibrated photodiode. The quantum yields were calculated without a correction for reflection and absorption.

Photovoltaic (PV) spectra of quantum well electrodes were measured by lock-in technique at room temperature under an illumination of 0.2−1.2 $\mu W/cm^2$ normalized monochromatic light of 850−1000 nm produced by a 250 W halogen tungsten

10.1021/jp9910542 CCC: $18.00
Published on Web 11/05/1999

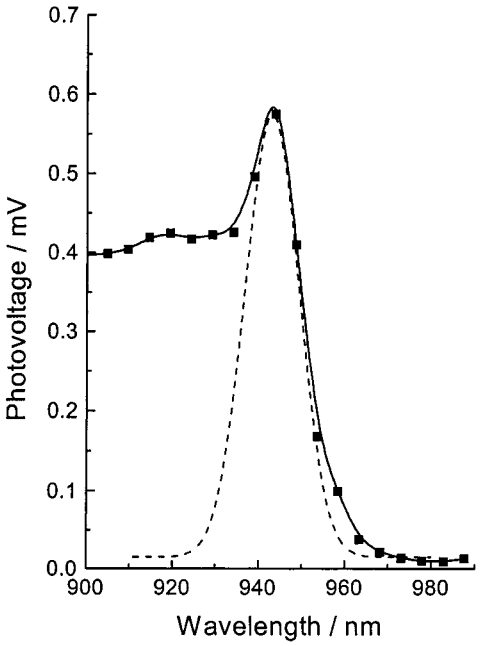

Figure 1. Photovoltaic spectrum of the strained $In_xGa_{1-x}As/GaAs$ double single-quantum-well electrode. The dashed line is a Gaussian line shape of exciton absorption.

lamp through a monochromator with a resolution of 4 nm. The chopper frequency was 22 Hz.

Results and Discussion

For a multiple quantum well photoelectrochemical electrode, each quantum well is located in a different region of the space charge layer. Therefore, the interfacial separation and transfer behaviors of photogenerated carriers in different wells may be different. Energy levels of carriers quantize when the size of semiconductor material is less than its Bohr's radius, forming a size-dependent exciton whose absorption is much stronger than the absorption of the free carrier. Excitonic absorption may be used to study the photoelectrochemical behavior of photogenerated carriers within the space charge layer under illumination with a suitable excitation wavelength. Herewith, a double single-quantum-well, located in different regions of the space charge layer, with different well widths was designed and fabricated in order to study the interfacial transfer behavior of carriers in the different quantum wells under a selective excitation.

Figure 1 presents the PV spectrum of the $In_{0.15}Ga_{0.85}As/GaAs$ DSQW electrode in the Fc/Fc^+ solution. Two photovoltaic structures, a peak located at 1.315 eV with fwhm (full width at half-maximum) of 18 meV and a small bulge at 1.351 eV, were resolved in the PV spectrum. For a semiconductor photovoltaic device, the photovoltage can be described as[21]

$$i_{ph} = i_0\left[\exp\left(\frac{neV_{ph}}{kT}\right) - 1\right] \quad (1)$$

where i_{ph} is the photocurrent, i_0 is the saturation current, V_{ph} is the open-circuit photovoltage, n is the ideal factor of photovoltaic devices, e is the electron charge, k is the Boltzmann constant, and T is the absolute temperature. In our case, the photovoltage of hundreds of microvolts generated at the incident intensity of 0.2−1.2 $\mu W/cm^2$ is much less than the value of kT/e (25 mV at room temperature). Hence the relationship of V_{ph} and I_{ph} shown in eq 1 can be approximated to a linear relation shown in eq 2. For a quantum well photoelectrode, when the quantum well thin layer is in the built-in electric field, the

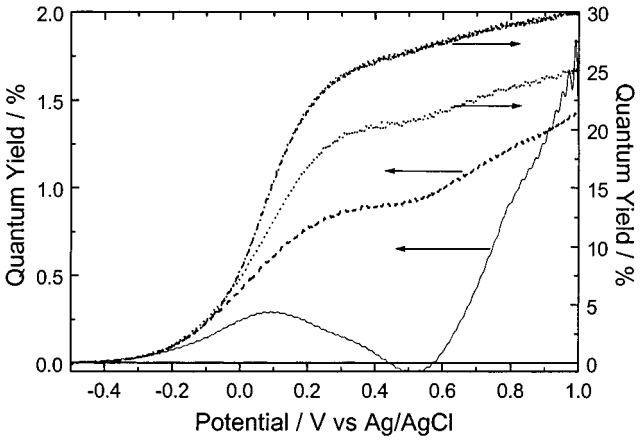

Figure 2. Plot of the quantum yield versus the electrode potential for the strained $In_xGa_{1-x}As/GaAs$ double single-quantum-well electrode excited under different wavelengths in contact with Fc/Fc^+ acetonitrile solution: (solid line) 950 nm; (dashed line) 900 nm; (dot line) 850 nm; (dot−dash line) 800 nm.

$$i_{ph} = i_0\frac{neV_{ph}}{kT} \quad (2)$$

photocurrent produced by the quantum well layer is described by[22]

$$i_{ph} = \frac{\lambda e}{hc}P_{in}\alpha(\lambda)L_w \quad (3)$$

where λ is the incident wavelength, c is the velocity of light, P_{in} is the incident intensity, $\alpha(\lambda)$ is the absorption coefficient at the wavelength λ, and L_w is the thickness of quantum well layer in the built-in field. Substituting (3) into (2), we get eq 4,

$$V_{ph} = \frac{kT\lambda}{nh^2ci_0}P_{in}\alpha(\lambda)L_w \quad (4)$$

in which, the photovoltage is proportional to the absorption coefficient of the quantum well. Thus, eq 4 can be used to describe the optical transitions in the quantum well. Taking into account the strain effect[23] and the band discontinuity (ΔE_C:ΔE_V = 9:1[24]), the theoretical transitions were calculated for a 9.8 nm $In_{0.15}Ga_{0.85}As/GaAs$ quantum well by using the finite square well model.[25] The transition energy from the first heavy hole level to the first electron level (H1E1) is 1.311 eV (946 nm). The transition energy from the first light hole level to the first electron level (L1E1) is 1.350 eV (919 nm). Comparison with these theoretical values, indicate that the sharp peak in Figure 1 stems from the H1El transition. For a $In_{0.15}Ga_{0.85}As/GaAs$ quantum well, the heavy hole and light hole are confined in different regions, i.e., the heavy hole in the $In_{0.15}Ga_{0.85}As$ layer (the same as electron) and the light hole in GaAs layer.[26] Owing to the large thickness of the GaAs layer, the confinement of the light hole is so weak that the bond of the light hole and electron is broken. The optical transition of the light hole shows a small hump instead of a sharp peak in the PV spectrum. The photoresponses of a 7.6 nm quantum well were not clearly observed. The theoretical transition energy of H1E1 for this narrow quantum well is 1.323 eV (937 nm). Because the 7.6 nm $In_xGa_{1-x}As$ quantum well is 400 nm away from the surface, it is located in a weak built-in electric field. The photovoltage produced by this quantum well may be quite small and does not make a pronounced contribution to the PV spectrum.

Figure 2 shows the photocurrent versus the electrode potential curves for a DSQW electrode illuminated by monochromatic

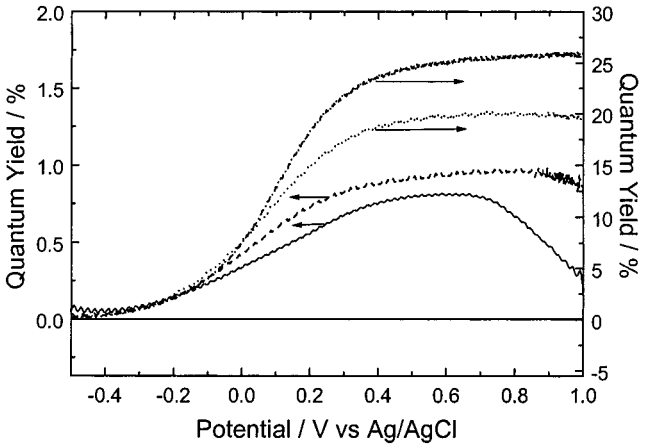

Figure 3. Plot of the quantum yield versus the electrode potential for the strained $In_xGa_{1-x}As$/GaAs double single-quantum-well electrode excited under different wavelengths in contact with $AcFc/AcFc^+$ acetonitrile solution: (solid line) 950 nm; (dash line) 900 nm; (dot line) 850 nm; (dot−dash line) 800 nm.

light with different wavelengths in the Fc/Fc^+ solution. It can be seen that, under the monochromatic light of 950 nm, the photocurrent increased with the positive shift of the bias, reaching an extremum at 0.1 V. Then it decreased to a minimum around 0.52 V and increased again at a more positive bias of 0.6 V. Similar phenomena were observed at the illumination of 900 nm wavelength. But the difference is that the minimum around 0.52 V is reduced to a small dip. In the case of the 850 nm illumination, which is able to excite the GaAs barrier layer ($E_g = 1.424$ eV, corresponding to a 870 nm absorption onset), the dip around 0.52 V in the photocurrent versus the electrode potential curve almost disappeared. With the illumination of 800 nm wavelength, which strongly excites the GaAs layer, the behavior of photocurrent versus bias resembled that of a bulk semiconductor electrode. The onset potentials of the photocurrent shown in Figure 2 for the excitations of different wavelengths were the same. The photocurrent gradually increased from the onset potential, showing a tardy photocurrent for all cases of illumination. Figure 3 illustrates the photocurrent characteristics of the DSQW electrode in $AcFc/AcFc^+$ solution. Comparing with Figure 2, the pronounced difference is that the position of the deep dip shifts to over 1.0 V in $AcFc/AcFc^+$ electrolyte in the case of 950 and 900 nm wavelength illumination.

As shown in Figures 2 and 3, the photocurrent of the quantum well is an anodic current that increased with the positive shift of the electrode potentials from the onset potential. The photogenerated hole transfers to the redox species in the electrolyte, and the electron flux drifts into the bulk of the electrode driven by the electric field of the space charge layer. With the increase of electrode potentials, the band bending increases, inducing a more efficient separation of electron−hole pairs and an increase in photocurrent, showing a behavior of n-type semiconductors. This is consistent with the n-type unintentional doping during the preparation of samples. In the case of 950 nm illumination, as indicated in Figure 1, the abnormal photocurrent behaviors indicate a special charge transfer occurring. Only 950 nm light can excite the 9.8 nm $In_{0.15}Ga_{0.85}As$ quantum well layer and mainly produce the electron−hole exciton. The bound exciton may slow the thermionic emission of carriers into the continuum of the energy band, which is a dominant way for separation of the electron−hole pair confined in the quantum well at room temperature.[27] The barrier potential of the $In_{0.15}Ga_{0.85}As$/GaAs quantum well

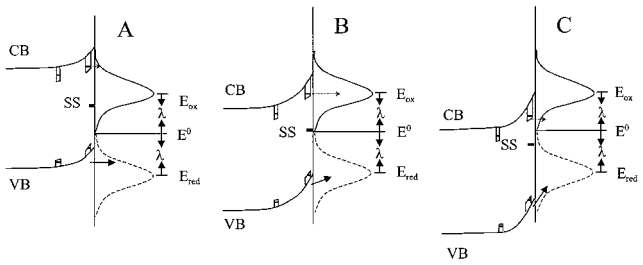

Figure 4. Band diagram of the quantum well electrode indicating the degree of overlap of the electron level with acceptor due to the band edge movement. CB is the conduction band of the semiconductor. VB is the valence band of the semiconductor. SS is the surface state. E_{ox} is the maximum density of occupied redox levels. E^0 is the normal redox potential of redox couple. E_{red} is the maximum density of empty redox levels. λ is the solvent reorganization energy. (A) Electrode potential less than 0.5 V. (B) Electrode potential around 0.5 V. (C) Electrode potential larger than 0.5 V.

was estimated to be 183 meV for the electron and 20 meV for the heavy hole. The heavy hole can absorb thermal energy to over the potential barrier into the continuum of the valence band. On the basis of the Franck−Condon principle, the electron confined to the deep potential well may tunnel into the acceptor state (Fc^+) of redox couples when the energy levels of the electron match the energy level of oxidized species, producing an extra cathodic current called the *photocathodic current* in this work. Hypothetically, the energy level of the electron matches the level of oxidized species due to a band edge movement when the electrode potential positively shifts to 0.1 V. The photocathodic current is produced through tunneling processes. The net photocurrent, a composite of photoanodic current and photocathodic current, decreases. The energy levels of electron and oxidized species are illustrated in Figure 4A. At 0.5 V, the overlap of the electronic wave function with the energy distribution of oxidized species reaches a maximum, as shown in Figure 4B, the photogenerated electron almost tunnels into the electrolyte, resulting in a zero net photocurrent. The tunneling probabilities of photogenerated electrons approach 100%. This can be thought of as an indirect recombination process via an interfacial tunneling electron transfer. The tunneling photocurrent produced by photogenerated electrons was also observed in a superlattice p-i-n diode.[28] The lifetime of thermionic emission for electrons confined in the studied quantum well was calculated to be ∼450 ps by using the thermionic emission model developed by Schneider and Klitzing.[29,30] The radiative lifetime of photogenerated carrier is hundreds to thousands of picoseconds for the (InGa)As/GaAs quantum well at room temperature.[31,32] This implies that the electron in the quantum well takes hundreds of picoseconds or less to tunnel into the acceptor state, faster than thermionic emission. The fast tunneling rate implies that defect-assisted resonant tunneling of the electron through the GaAs barrier may exist.

When the electrode potential increases further, the overlap of the electronic wave function with the energy distribution of oxidized species becomes poor (Figure 4C). The decrease of the photocathodic current due to tunneling interfacial electron transfer engenders the increase of the net photocurrent. The range of electrode potential for the photocathodic current to occur was about 0.8 V in Fc/Fc^+ solution. In $AcFc/AcFc^+$ solution, the normal redox potential of the electrolyte is 0.25 V more positive than that of the Fc/Fc^+ solution. The electrode potential for the maximum overlap of the electronic wave function with the energy of oxidized species shifts to positive.

In the case of the excitation wavelength of 900 nm, the free carrier and exciton are simultaneously produced. The free carrier is easily thermalized into the continuum of the GaAs band and separated by the electric field of the space charge layer. The yield of photocathodic current produced by tunneling interfacial transfer of electron thus decreases, leading to only a small dip in the photocurrent versus the electrode potential curve. For the excitation of 850 and 800 nm, the GaAs layer is excited. The stronger absorption of the thicker GaAs layer may conceal the photoresponse signal of the $In_xGa_{1-x}As$ quantum well, resulting in a behavior like the n-type bulk GaAs electrode.

The band edge movement, which is necessary for the energy level matching, is considered to arise from surface states. This can be understood as follows: The onset potentials of photocurrents were about −0.4 V vs Ag/AgCl in Fc/Fc^+ and $AcFc/AcFc^+$ electrolytes, as shown in Figures 2 and 3. This fact indicates that the Fermi level of the studied $In_{0.15}Ga_{0.85}As/GaAs$ quantum well electrode is pinned by the surface states. As we know, the wet etching results in a thickness fluctuation and a residual roughness of the surface at the outermost layer, which can influence the transition properties of a near surface quantum well.[33] Thus, no surface pretreatment was applied to the QW electrodes in this study. There was a 3 nm oxidized layer on the outermost GaAs surface of the studied QW electrodes detected by Auger electron spectroscopy and argon ion sputtering methods. According to the advanced unified defect model,[34,35] the antisite arsenic defects, with high concentration, act as main surface states on the GaAs surface. The surface states will result in a shift of the Helmholtz potential drop producing a band edge movement in a semiconductor/electrolyte system. The amount of band edge movement, ΔV_H, is determined by the fraction of charged surface states:

$$\Delta V_H = \frac{f N_{SS} e}{C_H} \tag{5}$$

where f is the fraction of occupied surface states, N_{SS} is the density of surface states, e is electron charge, and C_H is the capacitance of the Helmholtz layer. The applied potential, V, is the summation of both the potential drop in the space charge layer and in the Helmholtz layer, i.e., $V = \Delta V_{SC} + \Delta V_H$. As calculated in ref 10, a surface state density of $(1-2) \times 10^{13}$ cm^{-2} can induce a 0.3− 0.6 V band edge movement. Therefore, the surface states have a significant influence on the distribution of electrode potential.

In summary, we have experimentally studied the photovoltaic spectroscopic features and the relationship of the photocurrent to the electrode potential of $In_xGa_{1-x}As/GaAs$ QW electrodes in Fc and AcFc nonaqueous electrolyte. $In_xGa_{1-x}As/GaAs$ QW electrodes show a pronounced energy quantization effect at room temperature and a deep dip in the photocurrent−electrode potential curves. From the analysis of bias dependence of deep dips on the redox potential of electrolyte, we inferred that tunneling electron transfer occurred at the near surface quantum well−electrolyte interface.

Acknowledgment. This work was supported by the National Natural Sciences Foundation of China (Project No. 29603010) and Initiation Foundation of State Education Commission of China for Return-scholars. The facilities of Prof. S.-E. Lindquist's group at the Department of Physical Chemistry of Uppsala University were used in this work. Y.L. thanks Prof. S.-E. Lindquist for providing him a fellowship. The authors also would like to thank Dr. Yuan Lin for his useful discussions.

References and Notes

(1) Chang, L. L. In *Highlights in Condensed Matter Physics and Future Prospects*; Esaki, L., Eds.; Plenum: New York, 1991; p 83.
(2) Capasso, F. In *Physics and Applications of Quantum Wells and Superlattices*; Mendez, E. E., Von Klitzing, K., Eds.; Plenum: New York, 1987; p 377.
(3) Barnham K. W. J.; Duggan, G. *Appl. Phys. Lett.* **1990**, *67*, 3490.
(4) Paxman, M.; Nelson, J.; Braun, B.; Connolly, J.; Barnham, K. W. J.; Foxon, C. T.; Roberts, J. S. *J. Appl. Phys.* **1993**, *74*, 614.
(5) Barnham, K. W. J.; Braun, B.; Nelson, J.; Paxman, M. *Appl. Phys. Lett.* **1991**, *59*, 135.
(6) Anderson, N. G. *J. Appl. Phys.* **1995**, *78*, 1850.
(7) (a) Nozik, A. J.; Thacker, B. R.; Olson, J. M. *Nature* **1985**, *316*, 6023. (b) Nozik, A. J.; Thacker, B. R.; Olson, J. M. *Nature* **1987**, *326*, 450.
(8) Nozik, A. J.; Thacker, B. R.; Turner, J. A.; Olson, J. M. *J. Am. Chem. Soc.* **1985**, *107*, 7805.
(9) Nozik, A. J.; Thacker, B. R.; Turner, J. A.; Klem, J.; Morkoc, H. *Appl. Phys. Lett.* **1987**, *50*, 34.
(10) Nozik, A. J.; Thacker, B. R.; Peterson, M. W. *J. Phys. Chem.* **1988**, *92*, 2493.
(11) Nozik, A. J.; Thacker, B. R.; Turner, J. A.; Peterson, M. W. *J. Am. Chem. Soc.* **1988**, *110*, 7630.
(12) Parson, C. A.; Peterson, M. W.; Thacker, B. R.; Turner, J. A.; Nozik, A. J. *J. Phys. Chem.* **1990**, *94*, 3381.
(13) Parson, C. A.; Thacker, B. R.; Szmyd, D. M.; Peterson, M. W.; McMahon, W. E.; Nozik, A. J. *J. Chem. Phys.* **1990**, *93*, 7706.
(14) Nozik, A. J.; Ross, R. T. *J. Appl. Phys.* **1982**, *53*, 3813.
(15) Diol, S.; Poles, E.; Rosenwaks, Y.; Miller, R. J. D. *J. Phys. Chem. B* **1998**, *102*, 6193.
(16) Liu Y.; Xiao X. R.; Li X. P.; Xu, X. Z.; Yuan, Z. L.; Zeng, Y. P.; Yang, C. H.; Sun, D. Z. *J. Chem. Soc., Chem. Commun.* **1995**, 1439.
(17) Liu Y.; Xiao X. R.; Li X. P.; Xu, X. Z.; Yuan, Z. L.; Zeng, Y. P.; Yang, C. H.; Sun, D. Z. *J. Photochem. Photobiol. A: Chem.* **1997**, *101*, 113
(18) Liu Y.; Xiao X. R.; Xu, X. Z.; Yuan, Z. L.; Zeng, Y. P.; Yang, C. H.; Sun, D. Z. *Chem. Phys. Lett.* **1996**, *256*, 312.
(19) Liu Y.; Xiao X. R.; Wang, R. Z.; Li, D. L.; Zeng, Y. P.; Yang, C. H.; Sun, D. Z. *J. Electroanal. Electrochem.* **1997**, *430*, 91.
(20) Liu Y.; Xiao X. R.; Wang, R. Z.; Li, D. L.; Zeng, Y. P.; Yang, C. H.; Sun, D. Z. *J. Electroanal. Electrochem.* **1997**, *429*, 55.
(21) Pleskov, Yu. V.; Gurevich, Yu. Ya. In *Semiconductor Photoelectrochemistry*; Consultant Bureau, New York, 1986.
(22) Grahn, H. T.; Fischer, A.; Ploog, K. *Appl. Phys. Lett.* **1992**, *61*, 2211.
(23) Yeh, Y. H.; Lee, J. Y. *J. Appl. Phys.* **1997**, *81*, 6921.
(24) Lu, L. W.; Zhang, Y. H.; Yang, G. W.; Wang Z. G.; Wang, J.; Wang, Y.; Ge W. K. *Acta Phys. Sin.* **1998**, *47*, 1339.
(25) Kawai, H.; Kaneko, K.; Watanabe, N. *J. Appl. Phys.* **1984**, *56*, 463.
(26) Marzin, J. Y.; Chrasses, M. V.; Sermage, B. *Phys. Rev.* **1985**, *B31*, 8298.
(27) Nelson, J.; Paxman, M.; Barnham, K. W. J.; Roberts, J. S.; Button, C. *IEEE J. Quantum Electron.* **1993**, *29*, 1460.
(28) Tarucha, S.; Ploog, K. *Phys. Rev. B* **1989**, *39*, 5353.
(29) Schneider, H.; v. Klitzing, K. *Phys. Rev.* **1988**, *B38*, 6160.
(30) Fox, A. M.; Miller, D. A. B.; Livescu, G.; Cunningham, J. E.; Jan, W. Y. *IEEE J. Quantum Electron.* **1991**, *27*, 2281.
(31) Takahashi, K.; Owa, S.; Kano, S. S.; Muraki, K.; Fukatsu, S.; Shiraski, Y.; Ito, R. *Appl. Phys. Lett.* **1992**, *60*, 213.
(32) Xu, Z. Y.; Luo, C. P.; Jing, S. R.; Xu, J. Z.; Zheng, B. Z. *Chin. J. Semiconductors* **1995**, *16*, 101.
(33) Dreybrodt, J.; Forchel, A.; Reithmaier, J. P. *Phys. Rev.* **1993**, *B48*, 14741.
(34) Spicer W. E.; Liliental-Weber, Z.; Newman, N.; Kendelewicz, T.; Cao, R.; McCants, C.; Mahowald, P.; Miyano, K.; Lindau, I. *J. Vac. Sci. Technol.* **1988**, *B6*, 1245.
(35) Chiang, T. T.; Spindt, C. J.; Spicer W. E.; Lindau, I.; Browing, R. *J. Vac. Sci. Technol.* **1988**, *B6*, 1409.